



CHORUS

This is the accepted manuscript made available via CHORUS. The article has been published as:

Measurements of the $^{169}\text{Tm}(n,2n)^{168}\text{Tm}$ cross section from threshold to 15 MeV

J. Soter, M. Bhike, S. W. Finch, Krishichayan, and W. Tornow

Phys. Rev. C **96**, 064619 — Published 27 December 2017

DOI: [10.1103/PhysRevC.96.064619](https://doi.org/10.1103/PhysRevC.96.064619)

Measurements of the $^{169}\text{Tm}(n,2n)^{168}\text{Tm}$ cross section from threshold to 15 MeV

J. Soter,* M. Bhike, S.W. Finch, Krishichayan, and W. Tornow†

Department of Physics, Duke University
Durham, NC 27708 USA

Triangle Universities Nuclear Laboratory
Durham, NC 27708, USA

Measurements of the $^{169}\text{Tm}(n,2n)^{168}\text{Tm}$ cross section have been performed via the activation technique at 13 energies between 8.5 and 15.0 MeV. The purpose of this comprehensive data set is to provide an alternative diagnostic tool for obtaining subtle information on the neutron energy distribution produced in inertial confinement deuterium-tritium fusion experiments at the National Ignition Facility (NIF) at Lawrence Livermore National Laboratory. The $^{169}\text{Tm}(n,2n)^{168}\text{Tm}$ reaction not only provides the primary 14 MeV neutron fluence, but also the important down-scattered neutron fluence, the latter providing information on the density achieved in the deuterium-tritium plasma during a laser shot.

I. INTRODUCTION

For practical reasons monoisotopic chemical elements play an important role in applied nuclear physics. The rare earth element thulium with $Z = 63$ and $A = 169$ is no exception. Its $(n,2n)$ Q value of -8.1 MeV and the decay radiation of the daughter nucleus ^{168}Tm make thulium a convenient diagnostic tool for measuring the neutron fluence in laser shots at the National Ignition Facility (NIF), located at Lawrence Livermore National Laboratory. There deuterium-tritium (DT) loaded capsules are bombarded with powerful lasers with the goal of achieving ignition. Until now this goal has not been met, and efforts are underway to understand the complicated physics governing the plasma-laser interaction. Because of the high instantaneous neutron flux from the $d + T \rightarrow n + \alpha$ reaction, traditional neutron time-of-flight techniques employing even the fasted plastic scintillator based neutron detectors and associated photo-multiplier tubes reach the limits of their applicability. Therefore, passive methods for neutron fluence determination are an important alternative [1]. The $^{169}\text{Tm}(n,2n)^{168}\text{Tm}$ reaction probes the primary and down-scattered neutron energy spectrum from the $d + T \rightarrow n + \alpha$ reaction with maximum energy of 14.7 MeV. Because of the high deuterium, tritium, and neutron density within the DT plasma, there is a finite probability for secondary reactions, i.e., elastic and inelastic neutron scattering off deuterons and tritons, resulting in lower energy, so-called down-scattered neutrons [2]. Valuable information on the plasma density could be obtained if the $^{169}\text{Tm}(n,2n)^{168}\text{Tm}$ cross section is accurately known. Recent work [3, 4] has focused on the $^{169}\text{Tm}(n,3n)^{167}\text{Tm}$ reaction with a Q value of -15.0 MeV. This reaction probes the reaction-in-flight (RIF) neutrons, which could have energies up to 30 MeV [5]. Again, their fluence is a measure of the DT plasma density. Considerably stronger conclusions can be drawn, however, if both down-scattered and RIF neutron fluence can be measured simultaneously in the same laser shot. This is the main motivation for

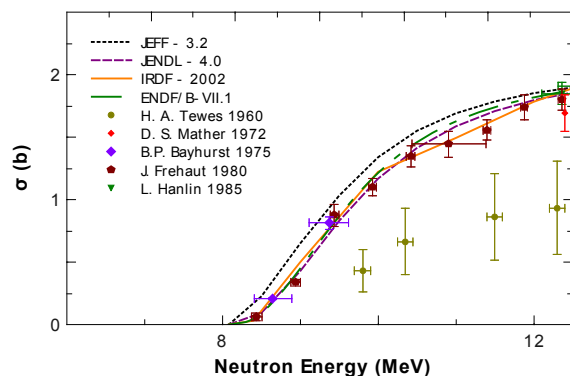


FIG. 1. (Color online) Available literature data and evaluations for the $^{169}\text{Tm}(n,2n)^{168}\text{Tm}$ cross section from threshold to 12.5 MeV. The horizontal error bars illustrate the spread of neutron energies used in the experiment.

the present $^{169}\text{Tm}(n,2n)^{168}\text{Tm}$ cross-section measurements.

The $^{169}\text{Tm}(n,2n)^{168}\text{Tm}$ cross section has been heavily investigated in the 14 MeV energy range. In contrast, data below this energy are scarce. Figure 1 shows the experimental information available for the $^{169}\text{Tm}(n,2n)^{168}\text{Tm}$ cross section from threshold up to 12.5 MeV in comparison to the commonly used nuclear data evaluations JEFF-3.2, JENDL-4.0 [6], IRDF-2002 and ENDF/B-VII.1 [7]. Focusing on this energy range, which is important to probe down-scattered neutrons at NIF, and ignoring the very early (1960) data of Tewes *et al.*, we note that in addition to the comprehensive data set of Frehaut *et al.* [8] there exist only two data points from Bayhurst *et al.* [9]. In contrast to the vast majority of $(n,2n)$ data reported in the literature, which are based on the well-known activation technique, Frehaut *et al.* detected the outgoing neutrons directly, using a sophisticated detector and analysis procedure, which have not been duplicated by any other group. The lack of sufficient $(n,2n)$ data below 12 MeV was one of the main reasons for the present study.

* REU student at TUNL from Drew University, summer 2016

† tornow@tunl.duke.edu

II. EXPERIMENTAL SETUP AND PROCEDURE

The experimental setup, data taking, and data analysis procedures are identical to those of Ref. [10]. In short, we used the neutron activation technique to measure the $^{169}\text{Tm}(n,2n)^{168}\text{Tm}$ cross section. The $^2\text{H}(d,n)^3\text{He}$ reaction was employed to produce mono-energetic neutrons in 0.5 MeV energy steps between 8.5 and 14 MeV. The $^{197}\text{Au}(n,2n)^{196}\text{Au}$ reaction served as neutron fluence monitor. In order to extend the energy range to higher energies, the $^3\text{H}(d,n)^4\text{He}$ reaction was used at 14.8 MeV. At such a high energy, the $^{169}\text{Tm}(n,2n)^{168}\text{Tm}$ and $^{197}\text{Au}(n,2n)^{196}\text{Au}$ reactions would be sensitive to so-called breakup neutrons from the $^2\text{H}(d,n)^3\text{He}$ reaction. In order to avoid making the associated corrections, the $^3\text{H}(d,n)^4\text{He}$ reaction with its large Q value of 17.59 MeV was employed. The TUNL tandem accelerator facility [11] provided and accelerated the deuteron beams. The thulium samples consisted of 11.1 mm diameter disks of 0.1 mm thickness. They were positioned at a distance of 2.5 cm from the end of the deuterium gas cell described in Ref. [12], or from the tritiated titanium target foil described in Ref. [13]. The thulium disks were sandwiched between two monitor foils of ^{197}Au of the same diameter as the thulium disks, and 0.025 mm thickness. Irradiation times varied between 2 hours and 8 hours, depending on neutron source reaction and energy. After irradiation the thulium and monitor foils were γ -ray counted in TUNL's Low-Background Counting Facility using 25%, 55%, or 60% relative efficiency (with respect to a $3'' \times 3''$ NaI detector) high-purity germanium (HPGe) detectors. The samples were positioned at a distance of 5.0 cm from the front face of the detectors. The γ -ray energies of interest and other relevant information are given in Table I for ^{169}Tm and ^{197}Au . The ^{168}Tm nucleus undergoes electron-capture to form ^{168}Er .

III. DATA ANALYSIS

Using the Canberra Multiport II data-acquisition system with associated GENIE software, the activity of the samples was followed until the initial activity was determined to sufficient accuracy. Figure 2 shows a γ -ray energy spectrum obtained at $E_n = 11.91$ MeV. For comparison, a background spectrum measured before irradiation is also shown, indicating a potential interference problem with an environmental background line in the case of the 184.3 keV transition in ^{168}Er . The well-known 355.73 keV neutron monitor transition in ^{196}Au was background free. Parts of the relevant level scheme of ^{168}Er are displayed in Fig. 3. As can be seen, ^{168}Er has strong γ -ray transitions. Figure 4 shows typical decay curves at selected incident neutron energies for ^{168}Tm and ^{196}Au . Within uncertainties, the measured decay half-times $T_{1/2}$ agree with the literature values.

The photo-peak efficiency of the HPGe detectors used in the present work was determined with calibrated test sources. Typical efficiency data and associated fit results are shown in Fig. 5.

In order to obtain the cross-section values of interest, the

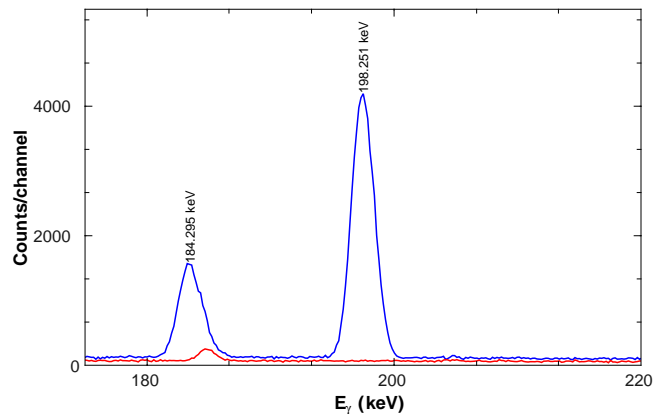


FIG. 2. (Color online) γ -ray energy spectra, expanded around the 200 keV region, obtained with a HPGe detector after five hours irradiation with a 11.91 ± 0.11 MeV neutron beam. The activated sample spectra is shown in blue and the background spectrum, measured before irradiation, is shown in red.

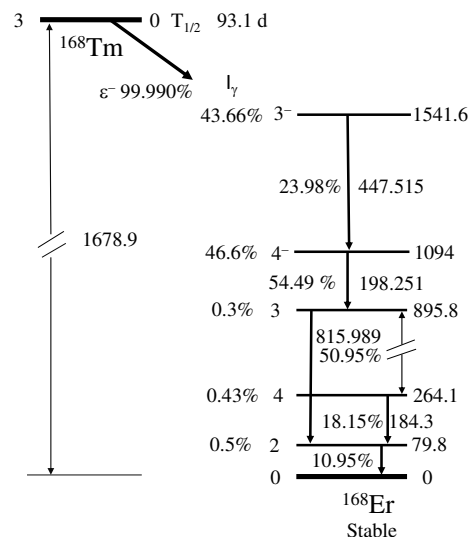


FIG. 3. Partial level scheme for decay of ^{168}Tm , showing all transitions measured in the present work. All energies are given in keV. Data taken from Ref. [14].

activation formula [15] is first used to obtain the neutron flux ϕ_n from the measured activity of ^{196}Au ,

$$\phi_n = \frac{A\lambda}{N\sigma\epsilon I_\gamma(1 - e^{-\lambda t_i})e^{-\lambda t_d}(1 - e^{-\lambda t_m})}, \quad (1)$$

where the induced activity A is the total yield in the photo-peak, N is the total number of target nuclei, ϵ is the photo-peak efficiency for the γ -ray energy of interest, I_γ is its intensity, t_i is the irradiation time, t_d is the decay time between the end of irradiation and the begin of off-line counting, t_m is the measuring time. The cross-section values, σ , for the $^{197}\text{Au}(n,2n)^{196}\text{Au}$ reaction were taken from Ref. [16].

Next, the activation formula is employed once more, this time with the induced activity of the ^{169}Tm foils

TABLE I. Relevant data for the reactions of interest in the present work

Reaction	Threshold [MeV]	Half-Life	Isotopic Abundance	E_γ [keV]	I_γ [%]
$^{169}\text{Tm}(n, 2n)^{168}\text{Tm}$	8.082	93.1 (2) d	100	184.295 (2)	18.15 (16)
				198.251 (2)	54.49 (16)
				447.515 (3)	23.98 (11)
				815.989 (5)	50.95 (16)
$^{197}\text{Au}(n, 2n)^{196}\text{Au}$	8.114	6.1669 (6) d	100	355.73 (5)	87

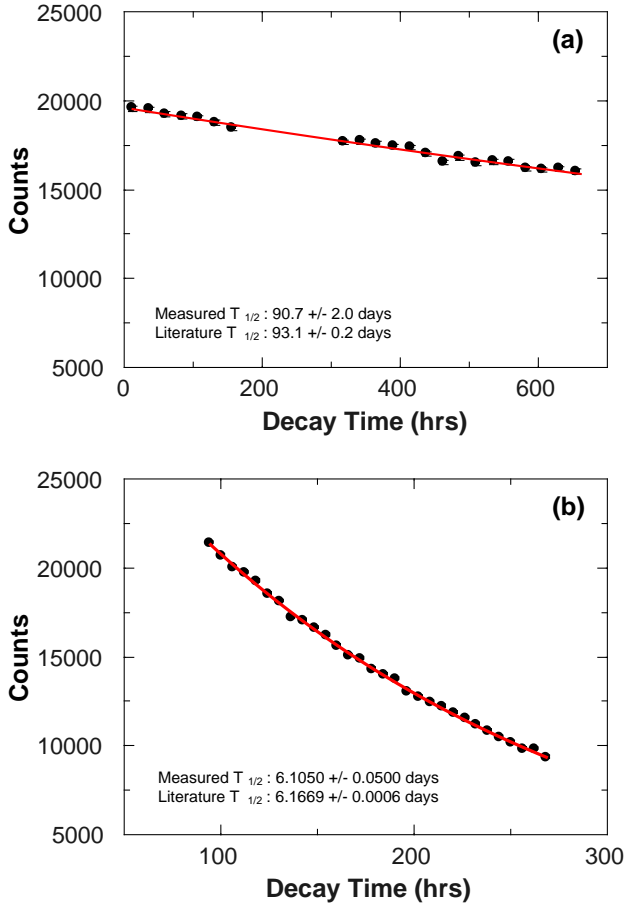


FIG. 4. (Color online) Measured decay curves of the (a) ^{168}Tm 198 keV activity after irradiation with 12.41 MeV neutrons and (b) ^{196}Au 355 keV activity after irradiation with 12.90 MeV neutrons. The data are fit to an exponential decay (red curves).

and ϕ_n obtained as described above, to determine the $^{169}\text{Tm}(n, 2n)^{168}\text{Tm}$ cross section of interest:

$$\sigma = \frac{A\lambda}{N\phi_n \epsilon I_\gamma (1 - e^{-\lambda t_i}) e^{-\lambda t_d} (1 - e^{-\lambda t_m})}, \quad (2)$$

where the notations follow those of Eq. (1).

We restricted ourselves to the strongest (198.251 keV) transition. As pointed out already, the 184.295 keV transition is affected by a background line. The 815.989 keV γ -ray has a similar intensity as the 198.251 keV transition, but its de-

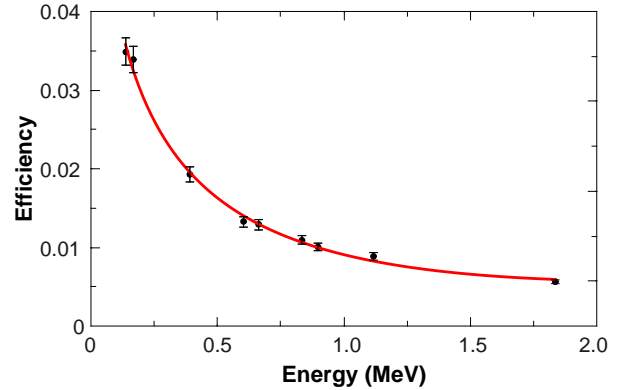


FIG. 5. (Color online) Measured efficiency data and fit (red curve) using a mixed γ -ray source positioned 5 cm away from the face of a 55% relative efficiency HPGe detector. The efficiency was fit to a function of the form $\sum_{i=0}^3 \epsilon_i \ln(E)^i$, where ϵ_i are free parameters.

tection efficiency is more than a factor of three lower than that of the 198.251 keV. The transitions at 447.515 keV and 815.989 keV also required larger summing corrections than the 198.251 keV γ -ray line. The coincidence summing corrections for the 198.251 keV transition varied between 1.5% and 4.5%, depending on the HPGe detector used to record the induced activity. The summing correction was confirmed by taking data with the same sample at 5 cm and 15 cm from the detector face. This was easily achievable given the long-lived activity of ^{168}Tm . For measurements made at a 15 cm distance, summing effects were found to be negligible. When determining final cross-section values, the summing effects were corrected for accordingly.

It should also be noted that the 447.515 keV transition yield consistently gave smaller cross-section values than the 198.251 or 815.989 keV transitions, indicating a problem with the published I_γ value. With the sample positioned 15 cm from the detector, the intensity ratio of the two strongest γ -ray transitions in ^{168}Er , 198.251 keV and 815.989 keV, was consistent with the literature value [14], within our experimental uncertainties. The intensity ratio of the 198.251 keV γ ray and the third strongest transition at 447.515 keV, however, was measured to be 2.60 ± 0.08 , in contrast to the literature intensity ratio of 2.27 ± 0.02 .

TABLE II. $^{169}\text{Tm}(n,2n)^{168}\text{Tm}$ reaction: neutron energy and associated energy spread, $^{197}\text{Au}(n,2n)^{196}\text{Au}$ reaction cross-section data used for determining the neutron fluence, and cross-section results obtained for the $^{169}\text{Tm}(n,2n)^{168}\text{Tm}$ reaction

Neutron energy [MeV]	Monitor σ [mb]	$^{169}\text{Tm}(n,2n)^{168}\text{Tm}$ σ [mb]
8.43 ± 0.12	77.85 ± 6.34	133.4 ± 12.4
8.93 ± 0.12	304.9 ± 11.8	401.3 ± 23.9
9.43 ± 0.12	651.5 ± 21.8	825.0 ± 56.6
9.93 ± 0.11	978.8 ± 29.7	1149.3 ± 74.4
10.42 ± 0.10	1222.1 ± 35.8	1321.9 ± 78.5
10.92 ± 0.12	1420.8 ± 39.2	1467.1 ± 53.6
11.41 ± 0.11	1577.6 ± 41.9	1584.3 ± 66.0
11.91 ± 0.11	1713.3 ± 43.6	1697.4 ± 69.3
12.41 ± 0.11	1834.6 ± 43.9	1807.6 ± 69.7
12.90 ± 0.10	1944.1 ± 41.7	1923.6 ± 68.4
13.40 ± 0.10	2043.7 ± 34.2	1982.4 ± 68.6
13.90 ± 0.09	2119.9 ± 25.3	2058.4 ± 67.1
14.80 ± 0.06	2164.2 ± 22.8	2068.2 ± 70.9

IV. RESULTS

Results for the $^{169}\text{Tm}(n,2n)^{168}\text{Tm}$ reaction cross section are shown in Fig. 6 in comparison to the existing data and evaluations. Our data confirm those of Frehaut *et al.*, the only previously available comprehensive data set below 12 MeV neutron energy, as well as the two data points of Bayhurst *et al.* With our improved accuracy, the $^{169}\text{Tm}(n,2n)^{168}\text{Tm}$ cross section is now very well determined in this energy range above the reaction threshold. At higher energies our data agree very well with the average of the existing data in the 13 to 15 MeV energy region. The existing evaluations all meet at 14 MeV. The largest difference between them can be seen in the 11 MeV energy region. Here the IRDF-2002 evaluation follows the trend of the experimental data, while the JENDL-4.0 and ENDF/B-VII.1 evaluations are somewhat higher in the 11 MeV to 12 MeV energy range. There is hardly any difference between the JENDL-4.0 and ENDF/B-VII.1 evaluations. The JEFF-3.2 evaluation over estimates all data below 12 MeV.

An excellent agreement was found using the TALYS-based evaluated nuclear data library (TENDL-2015) [17]. TENDL uses the output of the TALYS nuclear model calculation and is shown in Fig. 7, along with the present data. The largest deviation between our data and TALYS comes near threshold at the 8.43 MeV data point. Otherwise, the excellent agreement indicates that cross-section data are well modeled by TALYS and the default parameters are well chosen in this mass range.

Our results are presented in numerical form in Table II. The first column gives the mean neutron energy. The second column provides the monitor reaction cross-section data used to obtain the results given in column 3 for the $^{169}\text{Tm}(n,2n)^{168}\text{Tm}$ cross section. The uncertainty budget is summarized in Table III.

TABLE III. Uncertainty budget

Uncertainty	Tm [%]	Monitors [%]
Counting statistics	0.1-1.6	0.03-0.60
Reference cross section	-	1.1-8.1
Detector Efficiency	0.81-7.77	2.4-4.8
Half-life	0.21	0.01
γ -ray intensity	-	0.29
Coincidence summing	3-5	1-3
Source geometry and Self-absorption of γ rays	<0.5	<0.5
Irradiation time	<0.5	<0.5
Decay time	<0.5	<0.5
Counting time	<0.5	<0.5
Neutron flux fluctuation	<0.5	<0.5

V. CONCLUSION

This work presents an accurate and comprehensive cross-section data set for the $^{169}\text{Tm}(n,2n)^{168}\text{Tm}$ reaction from threshold to 15 MeV. The present data favor the IRDF-2002, ENDF/B-VII.1 and JENDL-4.0 evaluations over those of JEFF-3.2. The results of our measurements provide an improved basis for determining the down-scattered neutron fluence component obtained in laser shots on DT capsules at NIF. This diagnostic tool is expected to give valuable information on the density of the inertial confinement fusion plasma.

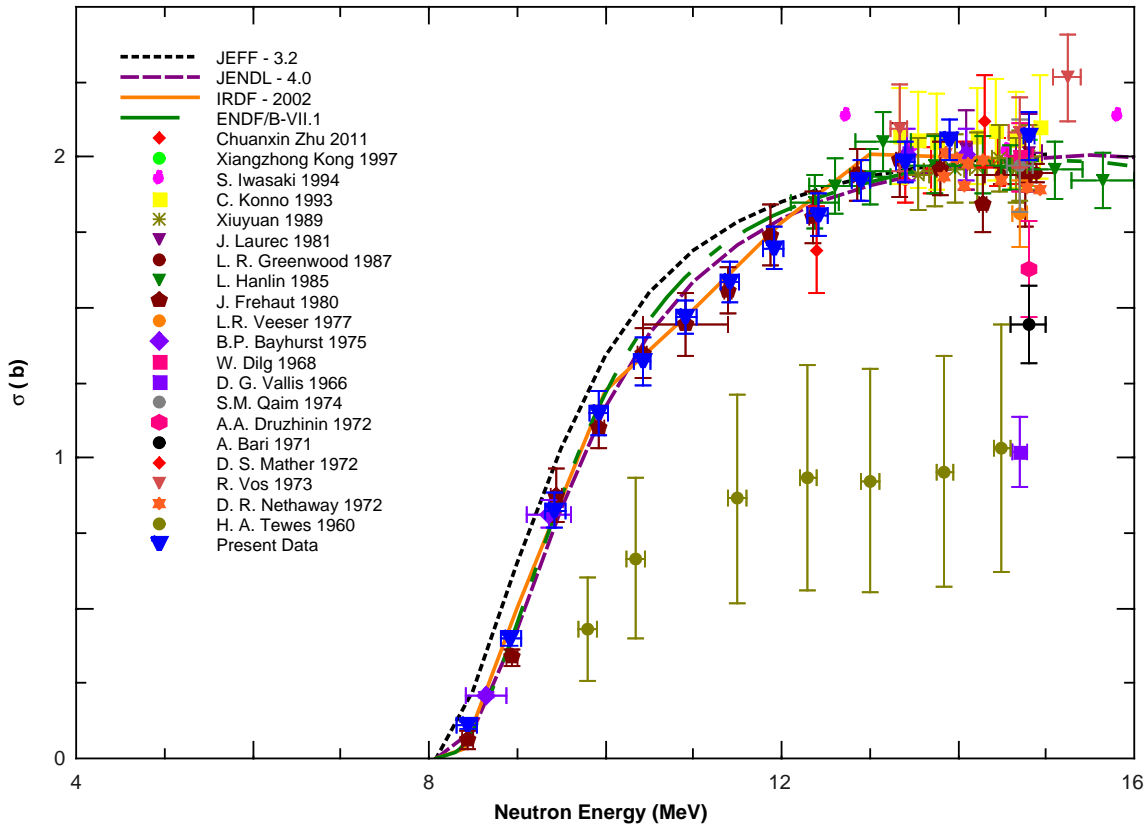


FIG. 6. (Color online) $^{169}\text{Tm}(n, 2n)^{168}\text{Tm}$ cross-section data in comparison to evaluations and previous data. The horizontal error bars indicate the neutron energy spread for the present experiment.

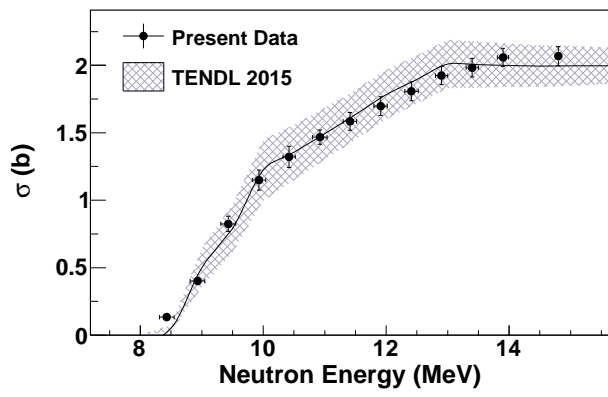


FIG. 7. (Color online) The present data compared with the TENDL-2015 output of the TALYS calculation. The calculation with the default parameters is shown by the solid black curve, with the shaded region showing the range of results achieved by varying the parameters.

ACKNOWLEDGMENTS

This work was supported in part by the National Nuclear Security Administration under grant no. DE-NA0002936, and

the U.S. Department of Energy, Office of Nuclear Physics, under grant no. DE-FG02-97ER41033. J. Soter acknowledges support from the NSF Research Experience for Undergraduate (REU) students program, under grant no. NSF-PHY-1461204.

-
- [1] J. Frenje *et al.*, Nuclear Fusion **53**, 043014 (2013).
- [2] P. A. Bradley, G. P. Grim, A. C. Hayes, G. Jungman, R. S. Rundberg, J. B. Wilhelmy, G. M. Hale, and R. C. Korzekwa, Phys. Rev. C **86**, 014617 (2012).
- [3] B. Champine, M. E. Gooden, Krishichayan, E. B. Norman, N. D. Scielzo, M. A. Stoyer, K. J. Thomas, A. P. Tonchev, W. Tornow, and B. S. Wang, Phys. Rev. C **93**, 014611 (2016).
- [4] M. E. Gooden, T. A. Bredeweg, B. Champine, D. C. Combs, S. Finch, A. Hayes-Sterbenz, E. Henry, Krishichayan, R. Rundberg, W. Tornow, J. Wilhelmy, and C. Yeamans, Phys. Rev. C **96**, 024622 (2017).
- [5] J. Lindl, O. Landen, J. Edwards, and E. Moses, Physics of Plasmas **21**, 020501 (2014).
- [6] K. Shibata *et al.*, Journal of Nuclear Science and Technology **48**, 1 (2011).
- [7] M. Chadwick *et al.*, Nuclear Data Sheets **112**, 2887 (2011), special Issue on ENDF/B-VII.1 Library.
- [8] J. Frehaut, A. Bertin, R. Bois, and J. Jary, .
- [9] B. P. Bayhurst, J. S. Gilmore, R. J. Prestwood, J. B. Wilhelmy, N. Jarmie, B. H. Erkkila, and R. A. Hardekopf, Phys. Rev. C **12**, 451 (1975).
- [10] M. Bhike, B. Fallin, M. E. Gooden, N. Ludin, and W. Tornow, Phys. Rev. C **91**, 011601 (2015).
- [11] [Http://www.tunl.duke.edu/web.tunl.2011a.tandem.php](http://www.tunl.duke.edu/web.tunl.2011a.tandem.php).
- [12] C. Bhatia, S. W. Finch, M. E. Gooden, and W. Tornow, Phys. Rev. C **86**, 041602(R) (2012).
- [13] C. Bhatia, S. W. Finch, M. E. Gooden, and W. Tornow, Phys. Rev. C **87**, 011601(R) (2013).
- [14] [Http://www.nndc.bnl.gov/chart/](http://www.nndc.bnl.gov/chart/).
- [15] M. Bhike and W. Tornow, Phys. Rev. C **89**, 031602(R) (2014).
- [16] K. I. Zolotarev, INDC(NDS)-0526 (2008).
- [17] A. Koning and D. Rochman, Nuclear Data Sheets **113**, 2841 (2012), special Issue on Nuclear Reaction Data.